Journal of Machine Learning Research 9 (2008) 1583-1614 Submitted 9/07; Revised 1/08; Published 7/08

Dynamic Hierarchical Markov Random Fields for Integrated Web Data Extraction

Jun Zhu JUN-ZHU@MAILS.TSINGHUA.EDU.CN
Department of Computer Science and Technology
Tsinghua University
Beijing, 100084, China

Zaiqing Nie ZNIE@MICROSOFT.COM
Web Search and Mining Group
Microsoft Research Asia
Beijing, 100080, China

Bo Zhang DCSZB@TSINGHUA.EDU.CN
Department of Computer Science and Technology
Tsinghua University
Beijing, 100084, China

Ji-Rong Wen JRWEN@MICROSOFT.COM
Web Search and Mining Group
Microsoft Research Asia
Beijing, 100080, China

Editor: John Lafferty

Abstract

Existing template-independent web data extraction approaches adopt highly ineffective decoupled strategies—attempting to do data record detection and attribute labeling in two separate phases. In this paper, we propose an integrated web data extraction paradigm with hierarchical models. The proposed model is called Dynamic Hierarchical Markov Random Fields (DHMRFs). DHMRFs take structural uncertainty into consideration and define a joint distribution of both model structure and class labels. The joint distribution is an exponential family distribution. As a conditional model, DHMRFs relax the independence assumption as made in directed models. Since exact inference is intractable, a variational method is developed to learn the model's parameters and to find the MAP model structure and label assignments. We apply DHMRFs to a real-world web data extraction task. Experimental results show that: (1) integrated web data extraction models can achieve significant improvements on both record detection and attribute labeling compared to decoupled models; (2) in diverse web data extraction DHMRFs can potentially address the blocky artifact issue which is suffered by fixed-structured hierarchical models.

Keywords: conditional random fields, dynamic hierarchical Markov random fields, integrated web data extraction, statistical hierarchical modeling, blocky artifact issue

1. Introduction

The World Wide Web is a vast and rapidly growing repository of information. There are various kinds of objects, such as products, people, and conferences, embedded in webpages. Extracting object information is key to object-level search engines like *Libra* (http://libra.msra.cn/) and

Rexa (http://rexa.info). Recent work has shown that *template-independent* approaches to extracting meta-data for the same type of real-world objects are feasible and promising. However, existing approaches use highly ineffective decoupled strategies—attempting to do data record detection and attribute labeling in two separate phases. This paper is to first propose an integrated web data extraction paradigm with hierarchical Markov Random Fields, and then address the blocky artifact issue (Irving et al., 1997) with Dynamic Hierarchical Markov Random Fields.

A Motivating Example: we begin by illustrating the problem with an example, drawn from an actual application of product information extraction under our Windows Live Product Search project (http://products.live.com). The goal is to extract meta-data about real-world products from every product page on the Web. Specifically, for crawled webpages, we first use a classifier to select product pages and then extract the *Name*, *Image*, *Price*, and *Description* of each product from the identified product pages. Our statistical study on 51K randomly crawled webpages shows that about 12.6 percent are product pages. That is, there are about 1 billion product pages within a search index containing 9 billion crawled webpages. If only half of them are correctly extracted, we will have a huge collection of meta-data about real-world products that could be used for further knowledge discovery and data management tasks, such as comparison shopping and user intention detection.

However, how to extract product information from webpages generated by many (maybe tens of thousands of) different templates is non-trivial. One possible solution is that we first distinguish webpages generated by different templates, and then build an extractor for each template; this type of solution is *template-dependent*. Template-dependent methods are impractical for two reasons. First, accurately identifying webpages for each template is a far from trivial task because even webpages from the same website may be generated by dozens of templates. Second, even if we can distinguish webpages, the learning and maintenance of so many different extractors for different templates will require substantial efforts.

Fortunately, recent work (Lerman et al., 2004; Zhai and Liu, 2005; Zhu et al., 2005) has shown the feasibility and promise of *template-independent* meta-data extraction for the same type of objects. We can simply combine the existing techniques to build a template-independent extractor for product pages. Specifically, two types of webpages—*list pages* and *detail pages*[1]—are needed to be treated by existing extraction methods. List pages are webpages containing several structured data records, and detail pages are webpages only containing detailed information about a single object. Figure 1 illustrates these two types of pages. For list pages, we can first use the methods by Zhai and Liu (2005) Lerman et al. (2004) to detect data records and then use the model by Zhu et al. (2005) to label the data elements within the detected records. Similarly, for detail pages we can first use the methods by Song et al. (2004) to identify a main data block of a detail page, and then use the same model from Zhu et al. (2005) to do attribute labeling for the elements in the main block.

However, it is highly ineffective to use decoupled strategies—attempting to do data record detection and attribute labeling in two separate phases. The reasons for this are:

Error Propagation: as record detection and attribute labeling are two separate phases, the errors in record detection will be propagated to attribute labeling. Thus, the overall performance is limited and upper-bounded by that of record detection.

Lack of Semantics in Record Detection: human readers always take into account semantics of the text to understand webpages. For instance, in Figure 1(a), when claiming a block is a data record, we use the evidence that it contains a product's name, image, price, and description. Thus,

1. Our empirical study shows that about 0.35 of product pages are list pages and the rest are detail pages.

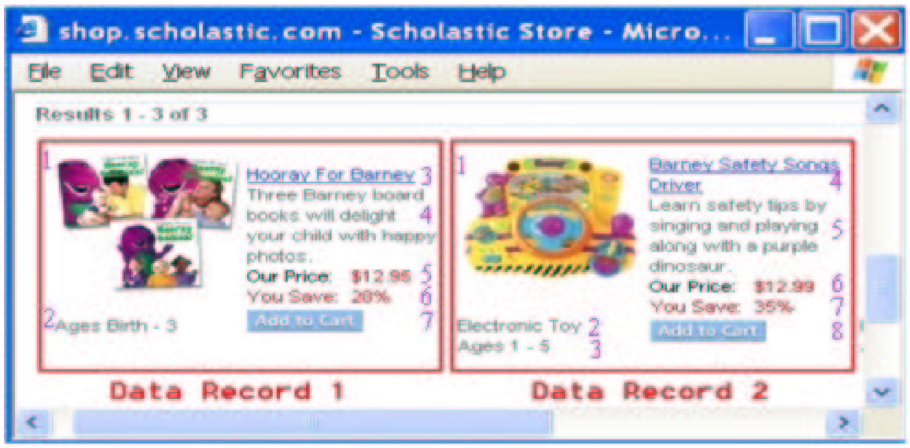
shop.scholastic.com - Scholastic Store - Micro...
File Edit View Favorites Tools Help
Results 1 - 3 of 3
1
Hooray For Barney 3
Three Barney board books will delight 4 your child with happy photos.
Our Price: $12.95 5
You Save: 28% 6
Add to Cart 7
2 Ages Birth - 3
1
Barney Safety Songs Driver 4
Learn safety tips by singing and playing 5 along with a purple dinosaur.
Our Price: $12.99 6
You Save: 35% 7
Add to Cart 8
Electronic Toy 2
Ages 1 - 5 3
Data Record 1
Data Record 2

(a) A list page with two data records. The first record contains 7 elements and the second contains 8 elements.

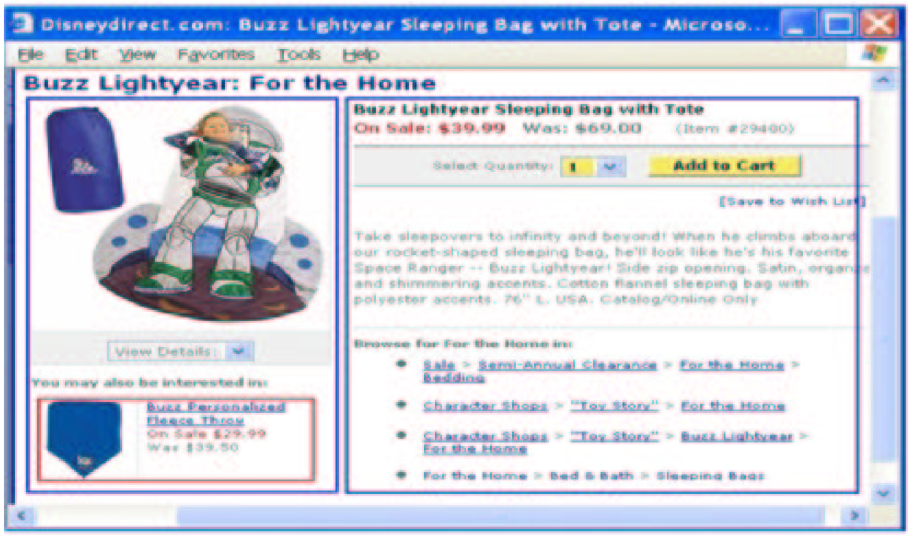
Disneydirect.com: Buzz Lightyear Sleeping Bag with Tote - Microso...
File Edit View Favorites Tools Help
Buzz Lightyear: For the Home
View Details
You may also be interested in:
Buzz Personalized Fleece Throw
On Sale $29.99
Was $39.50
Buzz Lightyear Sleeping Bag with Tote
On Sale: $39.99 Was: $69.00 (Item #29400)
Select Quantity: 1
Add to Cart
[Save to Wish List]
Take sleepovers to infinity and beyond! When he climbs aboard our rocket-shaped sleeping bag, he'll look like he's his favorite Space Ranger -- Buzz Lightyear! Side zip opening. Satin, organza and shimmering accents. Cotton flannel sleeping bag with polyester accents. 76" L. USA. Catalog/Online Only
Browse for For the Home in:
Sale > Semi-Annual Clearance > For the Home > Bedding
Character Shops > "Toy Story" > For the Home
Character Shops > "Toy Story" > Buzz Lightyear > For the Home
For the Home > Bed & Bath > Sleeping Bags

(b) A detail page contains one product item.

Figure 1: A sample list page and a detail page.

more effective record detection algorithms should take into account the semantic labels of the text, but existing methods (Zhai and Liu, 2005; Lerman et al., 2004) do not consider them.

Lack of Mutual Interactions in Attribute Labeling: data records in the same page are strongly correlated. They always have a similar layout and the elements at the same position of different records always have similar features and semantic labels. For example, in Figure 1(a) the element on the top-left of each record is an image. Existing methods (Zhu et al., 2005) do not achieve these correlations because data records are labeled independently.

First-Order Markov Assumption: for webpages, especially detail pages, long-distance dependencies always exist between different attribute elements. This is because there are always many irrelevant elements or noise elements appearing between the attributes. For example, in Figure 1(b) there are several noise elements, such as “Add to Cart” and “Select Quantity”, appearing between the price and description. However, plat models like 2D CRFs (Zhu et al., 2005) cannot incorporate long-distance dependencies because of their first-order Markov assumption.

To address the above problems, the first part of this paper is to propose an integrated web data extraction paradigm. Specifically, we take a vision-tree representation of webpages and define both record detection and attribute labeling as assigning semantic labels to the nodes on the trees. Then, we can define the integrated web data extraction that performs record detection and attribute labeling simultaneously. Based on the tree representation, we define a simple integrated web data extraction model—Hierarchical Conditional Random Fields (HCRFs), whose structures are determined by vision-trees.

However, for HCRFs, their structures may not be the most appropriate for web data extraction. This is because when constructing the vision-tree of each webpage, it is unaware of semantic labels. Thus, they cannot resolve all ambiguities. This will lead to those cases in which some closely related nodes may be separated significantly and only connected through a remote ancestor node on the tree. Due to the model’s local Markov assumption, it will lose some useful dependencies and result in low accuracy. An extreme case is that the attributes of different objects are intertwined. Figure 2 shows an example where the two neighboring records on the webpage have their attributes intertwined on the corresponding tree. In this case, fixed-structured hierarchical models are incapable of re-organizing them correctly. This problem has been generally known as blocky artifact issue in image processing (Irving et al., 1997).

Thus, effective web data extraction models should have the capability to adapt their structures during the inference process. The second part of this paper is to generalize Hierarchical Conditional Random Fields to incorporate structural uncertainty. The general model is called Dynamic Hierarchical Markov Random Fields (DHMRFs). DHMRFs consist of two parts—structure model and class label model. Both parts are jointly defined as an exponential family distribution. Compared to the directed Dynamic Trees (Williams and Adams, 1999) which have been proposed in image processing to address the blocky artifact issue, our model representation is compact and parameter sharing is easy. This is because conditional probability tables (CPTs) are used in Dynamic Trees to represent transition from parent nodes to child nodes. If different CPTs are used for different nodes, it will easily lead to over-parameterization. Thus, layer-wise CPT sharing is always adopted. But in the scenario of web data, sharing CPTs can be difficult because the hierarchical structures are not as regular as the dyadic or quad trees in image processing. Here, different pages can have quite different depths, and nodes from different pages at the same depth can have very diverse semantics. In contrast, DHMRFs define probability distributions via a set of feature functions and weights. These feature functions depend much more on observations and their labels than on the depths of the nodes. Thus, the undirected model is more suitable for diverse web data extraction. Furthermore, as a conditional model (Lafferty et al., 2001), DHMRFs relax the conditional independence assumption among observations as made in directed models. Finally, instead of trees in which only parent-child dependencies are assumed, DHMRFs consider the triple-wise interactions among neighboring sibling variables and their parent. These triple-wise dependencies provide more flexibility in encoding useful features.

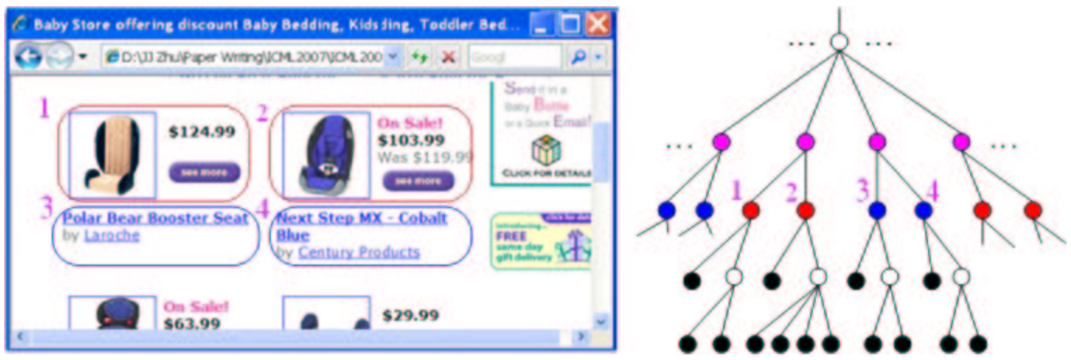

Figure 2: An intertwined example webpage. Blocks 1 and 3 present information of one product and blocks 2 and 4 present information of another product. But on the right tree, the information is not correctly grouped.

In undirected dynamic models, parameter estimation is generally intractable, especially when there are hidden variables—both structures and inner variables are hidden in our study. We develop a variational algorithm within the paradigm of contrastive divergence mean field learning (Welling and Hinton, 2001) to do parameter estimation and to find the MAP assignment of labels and the most likely model structures. The performance of our models is demonstrated on a web data extraction task—production information extraction. The results show that: (1) integrated web data extraction models can significantly improve the performance of both record detection and attribute labeling compared to decoupled methods; (2) Dynamic Hierarchical Markov Random Fields can (partially) avoid the blocky artifact issue and achieve high extraction accuracy without tedious manual labeling of inner nodes, which is required in the learning of the fixed-structured models; (3) integrated extraction models can generalize well to unseen templates. Note that the model is general and could be applied to other fields. We leave further examinations as future work.

The rest of the paper is organized as follows. In the next section, we discuss some background knowledge on which this work is based. Section 3 presents an integrated web data extraction paradigm and fixed-structured Hierarchical Conditional Random Fields. Section 4 describes Dynamic Hierarchical Markov Random Fields, including an approximate inference algorithm. Section 5 describes implementation details and experimental setup on the task of product information extraction. Section 6 and 7 presents evaluation results. Section 8 brings this paper to a conclusion and some future research directions are discussed. Finally, we give our acknowledgements.

2. Preliminary Background Knowledge

The background knowledge, on which the following work is based, is from web data extraction and statistical hierarchical modeling. We introduce these two fields in turn.

2.1 Web Data Extraction

Web data extraction is an information extraction (IE) task that identifies information of interest from webpages. The difference of web data extraction from traditional IE is that various types of structural dependencies between HTML elements exist. For example, the HTML tag tree is itself hierarchical and each webpage is displayed as a two-dimensional image to readers. Leveraging the two-dimensional spatial information to extract web data has been studied (Zhu et al., 2005; Gatterbauer et al., 2007). This paper is to explore both hierarchical and two-dimensional spatial information for more effective web data extraction.

Wrapper learning approaches (Muslea et al., 2001; Kushmerick, 2000) are template-dependent. They take in some manually labeled webpages and learn some extraction rules (or wrappers). Since the learned wrappers can only be used to extract data from similar pages, maintaining the wrappers as web sites change will require substantial efforts. Furthermore, in wrapper learning users must provide explicit information about each template. So it will be expensive to train a system that extracts data from many web sites. The methods by Embley et al. (1999), Buttler et al. (2001), Chang and Lui (2001), Crescenzi et al. (2001) and Arasu and Garcia-Molina (2003) are also template-dependent, but they do not need labeled training data. They produce wrappers from a collection of similar webpages.

The methods by Zhai and Liu (2005), Lerman et al. (2004) and Gatterbauer et al. (2007) are template-independent. In work by Lerman et al. (2004), data on list pages are segmented using the information from their detail pages. The need of detail pages is a limitation because automatically identifying links that point to detail pages is non-trivial and there are also many pages that do not have detail pages behind them. Zhai and Liu (2005) proposed to detect data records using string matching and also some visual features to achieve better performance, but no semantics are considered. Like the work by Zhu et al. (2005), a general 2D visual model was proposed by Gatterbauer et al. (2007) to extract web tables. The data extracted by the methods of Zhai and Liu (2005), Lerman et al. (2004) and Gatterbauer et al. (2007) have no semantic labels. Our work (Zhu et al., 2005) is complementary to this and assigns semantic labels to the extracted data.

2.2 Statistical Hierarchical Modeling

Multi-scale or hierarchical statistical modeling has shown great promise in image labeling (Kato et al., 1993; Li et al., 2000; He et al., 2004; Kumar and Hebert, 2005) and human activity recognition (Liao et al., 2005). Based on whether data are observed at multiple scales, two scenarios exist in which hierarchical modeling is appropriate. First, data are observed at different spatial scales and a model is used to integrate information from the different scales. Second, data are observed only at the finest scale and a model is used to induce a particular process at that scale. The introduced intermediate processes or variables can incorporate more complex dependencies to help the target labeling. Another merit of hierarchical models is that they admit more efficient inference algorithms compared to flat models (Willsky, 2002).

Traditional hierarchical models always assume that model structures are fixed or can be constructed via some deterministic methods, such as sub-sampling of images (Li et al., 2000) and the minimum spanning tree algorithm (Quattoni et al., 2004) with a proper definition of distance. However, in many applications this assumption may not hold. For example, fixed models in image processing often lead to the blocky artifact issue, and the similar problem arises in web data extraction due to the diversity of web data. To address this problem some enhanced models have been proposed, such as the overlapping tree approach (Irving et al., 1997). Superior performance is achieved with the improvement of the descriptive component of the model. However, ultimate solutions should deal with the source of the blockiness—fixed model structures. Based on this intuition, Dynamic Trees (Williams and Adams, 1999) have been proposed, which also consist of two parts—model of structures and model of class labels. However, the difference between DHMRFs and Dynamic Trees is that DHMRFs are defined as exponential family distributions and thus admit several advantages as discussed in the introduction.

Incorporating evidence at various scales was examined in a generative manner by Todorovic and Nechyba (2005). But our model is discriminative and it can relax the independence assumption among evidence as made in generative models. This is the key idea underlying Conditional Random Fields (Lafferty et al., 2001), which have shown great promise in information extraction (Culotta et al., 2006; Zhu et al., 2005). Modeling structural uncertainty has also been studied in relational learning (Getoor et al., 2001). Here, we focus on modeling the structural uncertainty within independently and identically distributed samples.

Finally, the work has partially appeared in the conference papers Zhu et al. (2006) and Zhu et al. (2007b).

3. Integrated Web Data Extraction

In this section, we formally define the integrated web data extraction and also propose Hierarchical Conditional Random Fields (HCRFs) to perform that task.

3.1 Vision-Tree Representation

For web data extraction, the first thing is to find a good representation format for webpages. Good representation can make the extraction task easier and improve extraction accuracy. In most previous work, tag-tree, which is a natural representation of the tag structure, is commonly used to represent a webpage. However, as Cai et al. (2004) pointed out, tag-trees tend to reveal presentation structure rather than content structure, and are often not accurate enough to discriminate different semantic portions in a webpage. Moreover, since authors use different styles to compose webpages, tag-trees are often complex and diverse. To overcome these difficulties, Cai et al. (2004) proposed a vision-based page segmentation (VIPS) approach. VIPS makes use of page layout features such as font, color, and size to construct a vision-tree for a page. It first extracts all suitable nodes from the tag-tree and then finds separators between these nodes. Here, separators denote horizontal or vertical lines in a webpage that visually do not cross any node. Based on these separators, the vision-tree of the webpage is constructed. Each node on this tree represents a data region in the webpage, which is called a block. The root block represents the whole page. Each inner block is the aggregation of all its child blocks. All leaf blocks are atomic units (i.e., elements) and form a flat segmentation of the webpage. Since vision-tree can effectively keep related content together while separating semantically different blocks from one another, we use it as our data representation format. Figure 3(a) is a vision-tree for the page in Figure 1(a), where empty circles denote inner blocks and filled circles denote leaf blocks (elements). For simplicity, we only show a sub-tree which contains the two data records in Figure 1(a). A detailed example was provided by Cai et al. (2004).

3.2 Record Detection and Attribute Labeling

Based on the definition of vision-tree, we now formally define the concepts of record detection and attribute labeling.

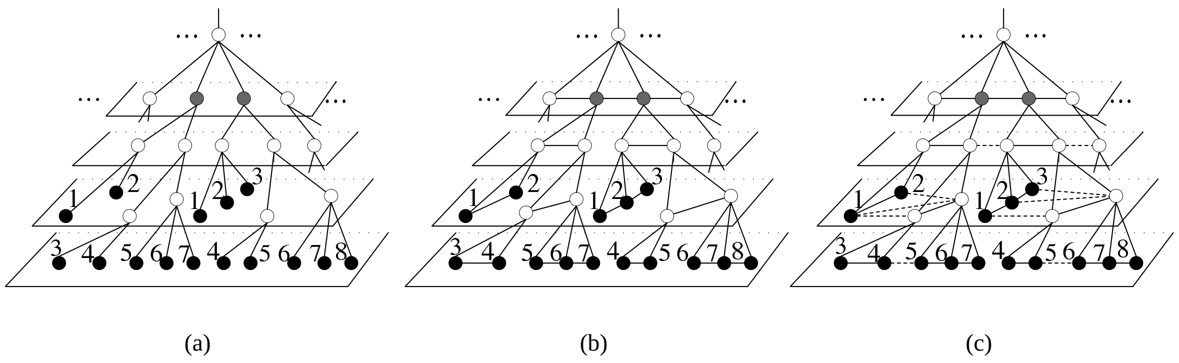

Figure 3: (a) Partial vision-tree of the webpage in Figure 1(a); (b) An HCRF model with linear-chain neighborhood between sibling nodes; (c) Another HCRF model with 2D neighborhood between sibling nodes and between nodes that share a grand-parent. Here, filled circles denote leaf blocks (elements) and the variables associated with them. Each filled circle corresponds to an element in the page in Figure 1(a) with the same number. Empty circles represent inner nodes and inner variables. The two gray nodes in each chart denote the roots of the sub-trees that correspond to the two data records in Figure 1(a).

Definition 3.1 (Record detection): Given a vision-tree, record detection is the task of locating the root of a minimal subtree that contains the content of a record. For a list page containing multiple records, all the records need to be identified.

For instance, for the vision-tree in Figure 3(a), the two blocks in gray are detected as data records. Note that as shown in Figure 2, given a particular vision-tree, we are not guaranteed to find the root nodes that correspond to data records. This is the very problem to be addressed by Dynamic Hierarchical Markov Random Fields.

Definition 3.2 (Attribute labeling): For each identified record, attribute labeling is the task of assigning attribute labels to the leaf blocks (elements) within the record.

We can build a complete model to extract both records and attributes by sequentially combining existing record detection and attribute labeling algorithms. However, as we have stated, this decoupled strategy is highly ineffective. Therefore, we propose an integrated approach that conducts simultaneous record extraction and attribute labeling.

3.3 Integrated Web Data Extraction

Based on the above definitions, both record detection and attribute labeling are the task of assigning labels to blocks of the vision-tree for a webpage. Therefore, we can define one probabilistic model to deal with both tasks. Formally, we define the integrated web data extraction as:

Definition 3.3 (Integrated Web Data Extraction): Given a vision-tree of a page, let $\mathrm{x} = \{x_0, x_1, \dots, x_N\}$ be the features of all the blocks and each component x_i is a feature vector of one block, and let $\mathrm{y} = \{y_0, y_1, \dots, y_N\}$ be one possible label assignment of the corresponding blocks. The goal of web data extraction is to find a label assignment $\mathrm{y}^\star$ that has the maximum posterior probability $\mathrm{y}^\star = \arg\max_{\mathrm{y}} p(\mathrm{y}|\mathrm{x})$, and extract data from this assignment.

3.4 Hierarchical Conditional Random Fields

In this section, we first introduce some basics of Conditional Random Fields and then propose Hierarchical Conditional Random Fields for integrated web data extraction.

3.4.1 CONDITIONAL RANDOM FIELDS

Conditional Random Fields (CRFs) (Lafferty et al., 2001) are Markov Random Fields that are globally conditioned on observations. Let $G = (V, E)$ be an undirected model over a set of random variables X and Y. X are variables over the observations to be labeled and Y are variables over the corresponding labels. The random variables Y could have a non-trivial structure, such as a linear-chain (Lafferty et al., 2001) and a 2D grid (Zhu et al., 2005). Each component Y_i has a label space or the set of possible labels $\mathcal{Y}_i$. The conditional distribution of the labels y (an instance of Y) given the observations x (an instance of X) has the form

$$p(\mathrm{y}|\mathrm{x}) = \frac{1}{Z(x)} \prod_{c \in \mathcal{C}} \phi(\mathrm{y}|_c, \mathrm{x}),$$

where $\mathcal{C}$ is the set of cliques in G; $\mathrm{y}|_c$ are the components of y associated with the clique c; ϕ is a potential function taking non-negative real values; $Z(\mathrm{x}) = \sum_{\mathrm{y}} \prod_{c \in \mathcal{C}} \phi(\mathrm{y}|_c, \mathrm{x})$ is the normalization factor or partition function in physics. The potential functions are usually expressed in terms of feature functions $f_k(\mathrm{y}|_c, \mathrm{x})$ and their weights λ_k:

$$\phi(\mathrm{y}|_c, \mathrm{x}) = \exp\left\{ \sum_k \lambda_k f_k(\mathrm{y}|_c, \mathrm{x}) \right\}.$$

Although functions f_k can take any real value, here we assume they are boolean and take either true or false.

3.4.2 HIERARCHICAL CONDITIONAL RANDOM FIELDS

Based on the vision-tree representation of the data, a Hierarchical Conditional Random Field (HCRF) model can be easily constructed. For the page in Figure 1(a) and its corresponding tree in Figure 3(a), an HCRF model is shown in Figure 3(b), where we also use empty circles to denote inner nodes and use filled circles to denote leaf nodes. For simplicity, only part of the model graph is presented. Each node on the graph is associated with a random variable Y_i. We will use nodes and variables exchangeably when there is no ambiguity. The observations that are globally conditioned on are omitted from this graph for simplicity. To make the model simple, we assume that the inner-layer interactions among sibling variables are sequential, that is, sibling variables are put into a sequence and only the relationships between neighboring variables are considered. Here, we use the position information and sequentialize the elements from left to right, top to bottom. For easy explanation and implementation, we assume that every inner node contains at least two children. Otherwise, we replace the parent with its single child. This assumption has no affect on the performance because the parent is identical to its child in this case.

The cliques of the graph in Figure 3(b) are its vertices, edges, and triangles. Let L be the number of layers indexed from 0 to $L-1$ starting from the root, and each layer $d (0 \leq d < L)$ has N_d nodes. Let s_{il} be an indicator variable to denote the connectivity between node i and node l, where l is at the direct above layer of i. Let n_{ij} be an indicator variable to denote whether node i and node j are adjacent to each other at the same layer. Then, $T = \cup_{d=1}^{L-1}\{(i,j,l) : 0 \leq i,j < N_d, 0 \leq l < N_{d-1}, n_{ij} = 1, s_{il} = 1, \textit{and } s_{jl} = 1\}$ is the set of triangles in the graph G. Thus, $\mathcal{C} = V \cup E \cup T$ and the conditional probability is

$$p(\mathrm{y}|\mathrm{x}) = \frac{1}{Z(x)} \exp\Big\{ \sum_{v \in V} \sum_k \mu_k g_k(\mathrm{y}|_v, \mathrm{x}) + \sum_{e \in E} \sum_k \lambda_k f_k(\mathrm{y}|_e, \mathrm{x}) + \sum_{t \in T} \sum_k \gamma_k h_k(\mathrm{y}|_t, \mathrm{x}) \Big\}.$$

Note that we use the same notation Z to denote the normalization factor for both CRFs and HCRFs, although they are different. We will follow this notation when there is no ambiguity in the rest of the paper.

Figure 3(c) presents another slightly more complicated HCRF model. In this model, we consider the two-dimensional inner-layer dependency relationships between sibling nodes. Moreover, we also consider the two-dimensional interactions between nodes that share a common grant-parent on the tree. In Figure 3(c), dotted edges are introduced to encode additional dependencies compared to the model in Figure 3(b). The conditional probability $p(\mathrm{y}|\mathrm{x})$ is the same as that of the previous model but with the dotted edges included in E.

For the model in Figure 3(b), the graph is a chordal graph and its inference can be exactly and efficiently done with the junction tree algorithm (Cowell et al., 1999). In fact, the complexity of the junction tree algorithm is linear in terms of the number of maximum cliques (or triangles), which can be shown to be equivalent to the number of leaf nodes (or elements). For the model in Figure 3(c), however, no exact inference algorithm exists; we have to turn to approximate algorithms. Since the backbone (without dotted edges) of the model graph is the same as the previous model, whose inference can be exactly done, piecewise learning (Sutton and McCallum, 2005) should be a good method. The basic idea of piecewise learning is to partition the graph into a set of disjointed small pieces. For each piece, exact inference can be efficiently done. Then, a lower bound of the log-likelihood function can be derived as the combination of the local log-likelihoods on different pieces. To use piecewise learning, here, we take the backbone as one piece and take each additional edge (a dotted edge) as one piece. The method by Wainwright et al. (2002) could be another excellent approximate algorithm in our model. Unlike piecewise learning whose parameter estimation is still a maximization problem, the parameter estimation by Wainwright et al. (2002) becomes a constrained saddle point problem.

4. Dynamic Hierarchical Markov Random Fields

In this section, we present the detailed description of Dynamic Hierarchical Markov Random Fields. An approximate inference algorithm is developed to perform parameter estimation and to find the maximum a posterior model structure and label assignment.

4.1 Model Description

Suppose we are given a set of N vertices, and each vertex is associated with a set of observations. Also suppose the vertices are arranged in a layered manner. Then, hierarchical statistical modeling is a task to construct an appropriate hierarchical model structure and carry out inference about the labels of given observations. Determining the number of layers and the number of nodes at each layer is problem specific. We will give an example of web data extraction in the experiment section. Let S be random variables over hierarchical structures, X be variables over the observations to be labeled, and Y be variables over the corresponding labels. Each component Y_i is assumed to take

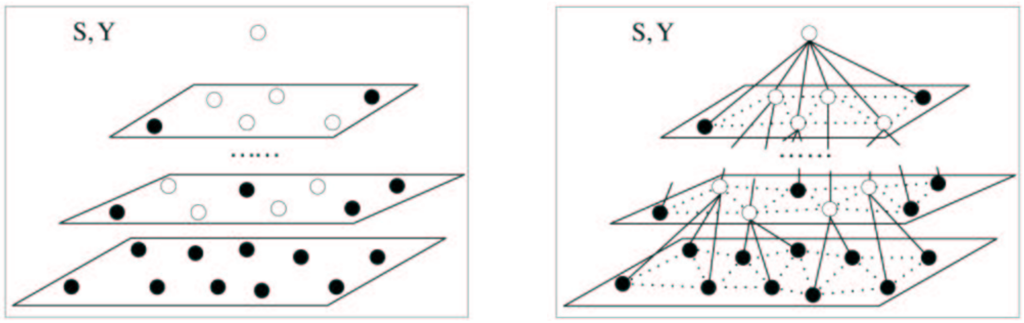

Figure 4: (a) The initial setting of DHMRFs with a set of nodes that are arranged in multi-layers. Filled circles denote leaf nodes or elements and empty circles denote inner blocks of a webpage; (b) An instance of DHMRFs denoted by S and Y. Vertical edges are selected by posterior probabilities $p(\mathrm{s}|\mathrm{x})$. Dotted lines represent the 2D neighborhood system between nodes at the same layer.

values from a finite discrete label space $\mathcal{Y}_i$. Here, capitalized characters denote random variables and corresponding lower cases are their instances or configurations, for example, y is a label assignment and $y_i \in \mathcal{Y}_i$ is one component label. A state of the system is the pairing of a model structure and a label assignment, that is, (s,y). Given observations x, Dynamic Hierarchical Markov Random Fields (DHMRFs) define a conditional probability distribution $p(\mathrm{s},\mathrm{y}|\mathrm{x})$ of structure s and label assignment y. An example is shown in Figure 4, where the left graph is the initial setting of DHMRFs with a set of nodes that are arranged in multi-layers and the right is an instance of the dynamic model. Let the energy of the system being at the state (s,y) be $E(\mathrm{s},\mathrm{y},\mathrm{x})$, then the probability of the system being at this state is

$$p(\mathrm{s},\mathrm{y}|\mathrm{x}) = \frac{1}{Z(\mathrm{x})}\exp\{-E(\mathrm{s},\mathrm{y},\mathrm{x})\}.$$

This is a Boltzmann distribution with the temperature $T = 1$, and our model is one type of exponential random graph model (Robins et al., 2006). Since the system consists of two parts, the energy is also from two parts. We explain them as follows:

Structure Model: Let s_{il} be an indicator variable to denote the connectivity between node i and another node l, which is at the direct above level. s_{il} equals to 1 if node i connects to node l; otherwise it is 0. Here, leaf nodes can be at any level except the root node that is taken as a default node for an entire page. For leaf nodes, no child is allowed. We call the parent-child connection *vertical connection*. To retain the computational advantage of tree-structured models, each node is allowed to have only one parent in a particular structure s. We will use s_v to denote the set of vertical connections. With the aforementioned definitions of L and N_d, we get $\mathrm{s}_v = \cup_{d=1}^{L-1}\{s_{il} : 0 \leq i < N_d \textit{ and } 0 \leq l < N_{d-1}\}$.

To consider the dependencies between the nodes at the same layer, *horizontal connection*s (i.e., connections between nodes at the same level) are incorporated in s. Let n_{ij} be an indicator variable to denote whether node i and node j are adjacent to each other. Similarly, n_{ij} equals to 1 if node

i connects to node j; otherwise, it is 0. Let's denote the set of horizontal connections by s_h, then $\mathrm{s}_h = \cup_{d=0}^{L-1}\{n_{ij} : 0 \leq i, j < N_d \textit{ and } i \neq j\}$. Here, we assume that the variables n_{ij} are independent of s_{il} and can be determined using some spatial ordering method. This assumption holds in applications such as web data extraction and image processing. As position information is encoded in each node, deterministic spatial ordering can decide the neighborhood system among a set of nodes. In theory, the horizontal neighborhood system can be arbitrary. We consider the 2D cases (Zhu et al., 2005), that is, each node is horizontally connected to all the nearest surrounding nodes in a 2D plane.

With the structure model, the first part of the energy when the system is at the state (s, y) is

$$E_1(\mathrm{s}, \mathrm{y}, \mathrm{x}) = \sum_k \mu_k \sum_{ijl} s_{il} s_{jl} n_{ij} g_k(i, j, l, \mathrm{x}),$$

where a triple (i, j, l) denotes a particular position in the dynamic model. A position can be a time interval in time series or a region of space in random fields. Here, i and j are two nodes at the same layer and l is a node at the direct above layer. g_k are feature functions defined on the three nodes at position (i, j, l), and μ_k are their weights.

Class Label Model: A sample s from the structure model defines a Hierarchical Conditional Random Field, which has been defined in Section 3.4.2. Let α_i^y be an indicator variable to denote the variable Y_i taking the class label y. Then, the second part of the energy when the system is at the state (s, y) is

$$E_2(\mathrm{s}, \mathrm{y}, \mathrm{x}) = \sum_k \lambda_k \sum_{ijl} s_{il} s_{jl} n_{ij} \sum_{y_i, y_j, y_l} \alpha_i^{y_i} \alpha_j^{y_j} \alpha_l^{y_l} f_k(y_i, y_j, y_l, \mathrm{x}),$$

where f_k are feature functions defined on the labels y_i, y_j, and y_l at position (i, j, l), and λ_k are their weights.

Although conditional models take observations as global conditions, when defining feature functions they need to know the "focused observations" at a particular position. For example, in linear-chain CRFs (Lafferty et al., 2001) the observation at time t is among the focused observations when defining feature functions related to the label y_t. In general, let t be a position and x_t be the set of focused observations at that position. The mapping function $\zeta : t \rightarrow \mathrm{x}_t$ defines the focused observations for each position. In generative models (Todorovic and Nechyba, 2005), the mapping function is defined to determine the observations generated by the states at a particular position. Moreover, an additional constraint $\forall t \neq s, \mathrm{x}_t \cap \mathrm{x}_s = \emptyset$ is also set due to their independence assumption that observations at different positions are conditionally independent given the states at those positions. In conditional models, however, there is no such constraint. The mapping function can be deterministic or stochastic. We assume it to be deterministic in this paper. Now, all feature functions take an additional argument ζ, that is, the feature functions are $g_k(i, j, l, \mathrm{x}, \zeta)$ and $f_k(y_i, y_j, y_l, \mathrm{x}, \zeta)$.

Taking E_1 and E_2 together, we get the joint distribution of s and y

$$p(\mathrm{s}, \mathrm{y}|\mathrm{x}) = \frac{1}{Z(\mathrm{x})} \exp\left\{ \begin{array}{c} \sum_k \mu_k \sum_{ijl} s_{il} s_{jl} n_{ij} g_k(i, j, l, \mathrm{x}, \zeta) + \\ \sum_k \lambda_k \sum_{ijl} s_{il} s_{jl} n_{ij} \sum_{y_i, y_j, y_l} \alpha_i^{y_i} \alpha_j^{y_j} \alpha_l^{y_l} f_k(y_i, y_j, y_l, \mathrm{x}, \zeta) \end{array} \right\},$$

where $Z(\mathrm{x})$ is the normalization factor or partition function in physics. Note that although names are similar, Dynamic Hierarchical Markov Random Fields are quite different from Dynamic CRFs (Sutton et al., 2004), which are dynamic in terms of time, that is, they have repetitive model structure and parameters over time, and the structure at each time slice is fixed. Here, "Dynamic" means the model's structure is dynamically selected.

4.2 Parameter Estimation and Labeling

Let $\Theta = \{\mu_1, \mu_2, \ldots; \lambda_1, \lambda_2, \ldots\}$ denote the whole set of the model's parameters, and let $D = \{(\mathrm{x}^i, \mathrm{y}_e^i)\}_{i=1}^K$ denote the set of training data, where x^i is a sample and y_e^i are observed labels. We consider the general case with both hidden hierarchical structure s and hidden labels y_h. For example, in web data extraction only the labels of leaf nodes are observable and both the hierarchical structures and the labels of inner nodes are hidden. So the log-likelihood of the data is incomplete

$$L(\Theta) = \sum_{i=1}^K \log p(\mathrm{y}_e^i|\mathrm{x}^i) = \sum_{i=1}^K \log(\sum_{\mathrm{s},\mathrm{y}_h} p(\mathrm{s}, \mathrm{y}_h, \mathrm{y}_e^i|\mathrm{x}^i)).$$

This function does not have a closed-form solution because of the marginalization taking place within the logarithm. In the following, we derive a lower bound of the log-likelihood, or equivalently an upper bound of the negative log-likelihood. Then, contrastive divergence learning (Hinton, 2002) is applied as an approximation.

Let $q(\mathrm{s}, \mathrm{y}_h|\mathrm{y}_e, \mathrm{x})$ be an approximation of the true distribution $p(\mathrm{s}, \mathrm{y}_h|\mathrm{y}_e, \mathrm{x})$. With a little abuse of notations, we will use $q(\mathrm{s}, \mathrm{y}_h)$ to denote $q(\mathrm{s}, \mathrm{y}_h|\mathrm{y}_e, \mathrm{x})$. We also ignore the summation operator in the log-likelihood during the following derivations, as there is no essential difference between one sample and a set of independently and identically distributed (IID) samples. The optimal approximation is the distribution that has the minimum Kullback-Leibler divergence between $q(\mathrm{s}, \mathrm{y}_h)$ and $p(\mathrm{s}, \mathrm{y}_h|\mathrm{y}_e, \mathrm{x})$. The KL divergence is defined as $KL(q||p) = \sum_{\mathrm{s},\mathrm{y}_h} q(\mathrm{s}, \mathrm{y}_h) \log \frac{q(\mathrm{s},\mathrm{y}_h)}{p(\mathrm{s},\mathrm{y}_h|\mathrm{y}_e,\mathrm{x})}$.

Take $p(\mathrm{s}, \mathrm{y}_h|\mathrm{y}_e, \mathrm{x}) = p(\mathrm{s}, \mathrm{y}_h, \mathrm{y}_e|\mathrm{x})/p(\mathrm{y}_e|\mathrm{x})$ into the above equation and use the non-negativity of KL divergence, we get a lower bound of the log-likelihood

$$\log p(\mathrm{y}_e|\mathrm{x}) \geq \sum_{\mathrm{s},\mathrm{y}_h} q(\mathrm{s}, \mathrm{y}_h)[\log p(\mathrm{s}, \mathrm{y}_h, \mathrm{y}_e|\mathrm{x}) - \log q(\mathrm{s}, \mathrm{y}_h)].$$

Equivalently, $\mathcal{L}(\Theta) \triangleq \sum_{\mathrm{s},\mathrm{y}_h} q(\mathrm{s}, \mathrm{y}_h)[\log q(\mathrm{s}, \mathrm{y}_h) - \log p(\mathrm{s}, \mathrm{y}_h, \mathrm{y}_e|\mathrm{x})]$ is an upper bound of the negative log-likelihood $-L(\Theta)$. By analogy with statistical physics, the upper bound, which is actually a KL divergence, can be expressed as the difference of two free energies: $\mathcal{L}(\Theta) = F_0 - F_\infty$, where the first term is the free energy when we use data distribution with observable labels clamped to their values, and the second $F_\infty = -\log Z(\mathrm{x})$ is the free energy when we use model distribution with all variables free.

Now, the problem is to minimize the upper bound. The derivatives of $\mathcal{L}(\Theta)$ with respect to λ_k are

$$\begin{aligned}
\frac{\partial \mathcal{L}(\Theta)}{\partial \lambda_k} &= \frac{\partial}{\partial \lambda_k} \langle -\log p(\mathrm{s}, \mathrm{y}_h, \mathrm{y}_e|\mathrm{x}) \rangle_{q(\mathrm{s},\mathrm{y}_h)} \\
&= -\sum_{ijl} \langle s_{il} s_{jl} n_{ij} \rangle_{q(\mathrm{s},\mathrm{y}_h)} \sum_{y_i, y_j, y_l} \langle \alpha_i^{y_i} \alpha_j^{y_j} \alpha_l^{y_l} \rangle_{q(\mathrm{s},\mathrm{y}_h)} f_k(y_i, y_j, y_l, \mathrm{x}, \zeta) - \frac{\partial F_\infty}{\partial \lambda_k} \\
&= -\sum_{ijl} n_{ij} \langle s_{il} s_{jl} \rangle_{q(\mathrm{s},\mathrm{y}_h)} \sum_{y_i, y_j, y_l} \langle \alpha_i^{y_i} \alpha_j^{y_j} \alpha_l^{y_l} \rangle_{q(\mathrm{s},\mathrm{y}_h)} f_k(y_i, y_j, y_l, \mathrm{x}, \zeta) - \frac{\partial F_\infty}{\partial \lambda_k},
\end{aligned} \tag{1}$$

where $\langle . \rangle_p$ is the expectation under the distribution p. The last equality holds because of the assumption that the neighborhood system between sibling nodes is determined independent of their parents.

Similarly, the derivatives of $\mathcal{L}(\Theta)$ with respect to μ_k are

$$\frac{\partial \mathcal{L}(\Theta)}{\partial \mu_k} = -\sum_{ijl} n_{ij} \langle s_{il} s_{jl} \rangle_{q(\mathrm{s},\mathrm{y}_h)} g_k(i,j,l,\mathrm{x},\zeta) - \frac{\partial F_\infty}{\partial \mu_k}. \tag{2}$$

In (1) and (2), the derivatives of the equilibrium free energy F_∞ are intractable in the case of Dynamic Hierarchical Markov Random Fields. However, by viewing the equilibrium distribution as the distribution of a Markov chain at time $t = \infty$ starting with data distribution, Markov chain Monte Carlo (MCMC) method can be used to reconstruct an approximation distribution $q_i(\mathrm{s},\mathrm{y}_h,\mathrm{y}_e)$ within several steps. This is the basic idea of contrastive divergence learning (Hinton, 2002). Now, the upper bound is approximated by

$$\begin{aligned}\mathcal{L}(\Theta) =& F_0 - F_\infty \\ &\approx F_0 - F_i = KL(q_0||p) - KL(q_i||p) \triangleq CF_i^{App},\end{aligned}$$

where $q_0 = q(\mathrm{s},\mathrm{y}_h)$ is optimized with observable labels clamped to their values, and $q_i(\mathrm{s},\mathrm{y}_h,\mathrm{y}_e)$ is optimized with all variables free starting with q_0. As shown by Hinton (2002), CF_i^{App}, known as contrastive divergence, is non-negative. But since $F_i \geq F_\infty$, there is no guarantee that it is still an upper bound. Some analyses of contrastive divergence learning (Yuille, 2004; Carreira-Perpinan and Hinton, 2005) have been carried out. In the sequel, we will set $i = 1$.

Now, the derivatives of CF_1^{App} with respect to the model's parameters are as in (1) and (2) but with the derivatives of F_∞ replaced by

$$-\sum_{ijl} n_{ij} \langle s_{il} s_{jl} \rangle_{q_1} \sum_{y_i y_j y_l} \langle \alpha_i^{y_i} \alpha_j^{y_j} \alpha_l^{y_l} \rangle_{q_1} f_k(y_i, y_j, y_l, \mathrm{x}, \zeta) \text{ and } -\sum_{ijl} n_{ij} \langle s_{il} s_{jl} \rangle_{q_1} g_k(i,j,l,\mathrm{x},\zeta)$$

respectively.

Generally, stochastic sampling is quite time demanding in constructing q_1. In contrast, the deterministic mean field variant (Welling and Hinton, 2001) is more efficient. An extension to the combination of a general deterministic variational approximation and contrastive divergence is studied by Welling and Sutton (2005). The learning procedure consists of two phases—wake phase and sleep phase. Wake phase is to optimize q_0 and sleep phase is to optimize q_1. We address the wake phase first.

Assume q_0 can be factorized as $q_0 = q(\mathrm{s},\mathrm{y}_h) = q(\mathrm{s})q(\mathrm{y}_h)$, and we get

$$KL(q_0||p) = -\langle \log p(\mathrm{s},\mathrm{y}_h,\mathrm{y}_e|\mathrm{x}) \rangle_{q_0} - H(q(\mathrm{s})) - H(q(\mathrm{y}_h)), \tag{3}$$

where $H(p) = -\langle \log p \rangle_p$ is the entropy of distribution p. To efficiently optimize q_0, more assumptions need to be made about the family of distributions of $q(\mathrm{s})$ and $q(\mathrm{y}_h)$. Here, we adopt the naïve mean field approximation. The basic idea underlying mean field theory (Jordan et al., 1999) is to make a distribution a factorized one by introducing additional independence assumptions. This factorized distribution leads to computational tractability. The simplest naïve mean field is to assume that interacted variables are mutually independent and the joint distribution is the product of single variable marginal probabilities.

Let μ_{il} be the probability of node i being connected to node l, and m_i^y be the probability of variable Y_i being at state y. As we assume variables n_{ij} are determined independent of s_{il}, the mean field distributions[2] are

$$q(\mathrm{s}) = \prod_{il} [\mu_{il}]^{s_{il}} \text{ and } q(\mathrm{y}_h) = \prod_{iy} [m_i^y]^{\alpha_i^y}.$$

Substitute the above distributions into (3) and keep $q(\mathrm{y}_h)$ fixed, then we get

$$KL(q_0||p) = -\langle \log p(\mathrm{s}, \mathrm{y}_h, \mathrm{y}_e|\mathrm{x})\rangle_{q_0} - H(q(\mathrm{s})) + c,$$

where c is a constant. Let the derivative over μ_{il} equal zero, and we get

$$\mu_{il} \propto \exp \left\{ \begin{array}{c} \sum_k \mu_k s_{il} \sum_j \langle s_{jl}\rangle_{q(\mathrm{s})} n_{ij} g_k(i,j,l,\mathrm{x}) + \\ \sum_k \lambda_k s_{il} \sum_j \langle s_{jl}\rangle_{q(\mathrm{s})} n_{ij} \sum_{y_1,y_2,y_3} \langle \alpha_i^{y_1}\alpha_j^{y_2}\alpha_l^{y_3}\rangle_{q(\mathrm{y}_h)} f_k(y_1,y_2,y_3,\mathrm{x},\zeta) \end{array} \right\}. \quad (4)$$

Normalization will lead to the desired probabilities μ_{il}.

Similarly, keep $q(\mathrm{s})$ fixed and we get

$$KL(q_0||p) = -\langle \log p(\mathrm{s}, \mathrm{y}_h, \mathrm{y}_e|\mathrm{x})\rangle_{q_0} - H(q(\mathrm{y}_h)) + c',$$

where c' is another constant. Let the derivative over m_i^y equal zero, and we get

$$m_i^y \propto \exp \sum_k \lambda_k \sum_{jly_1y_2} \left\{ \begin{array}{c} n_{ij}\langle s_{il}s_{jl}\rangle_{q(\mathrm{s})} \langle \alpha_j^{y_1}\alpha_l^{y_2}\rangle_{q(\mathrm{y}_h)} f_k(y,y_1,y_2,\mathrm{x},\zeta) + \\ n_{ij}\langle s_{jl}s_{il}\rangle_{q(\mathrm{s})} \langle \alpha_j^{y_1}\alpha_l^{y_2}\rangle_{q(\mathrm{y}_h)} f_k(y_1,y,y_2,\mathrm{x},\zeta) + \\ n_{jl}\langle s_{ji}s_{li}\rangle_{q(\mathrm{s})} \langle \alpha_j^{y_1}\alpha_l^{y_2}\rangle_{q(\mathrm{y}_h)} f_k(y_1,y_2,y,\mathrm{x},\zeta) \end{array} \right\}. \quad (5)$$

Note that since s_{il} and α_i^y are all indicator variables, their expectations are the marginal probabilities μ_{il} and m_i^y respectively. Also, because of the naïve mean field assumption of $q(\mathrm{s})$ and $q(\mathrm{y}_h)$, the expectations of the product of the indicator variables is the product of their corresponding marginal probabilities, that is, $\langle s_{il}s_{jl}\rangle_{q(\mathrm{s})} = \mu_{il}\mu_{jl}$, $\langle s_{ji}s_{li}\rangle_{q(\mathrm{s})} = \mu_{ji}\mu_{li}$, $\langle \alpha_j^{y_1}\alpha_l^{y_2}\rangle_{q(\mathrm{y}_h)} = m_j^{y_1}m_l^{y_2}$, and $\langle \alpha_i^{y_1}\alpha_j^{y_2}\alpha_l^{y_3}\rangle_{q(\mathrm{y}_h)} = m_i^{y_1}m_j^{y_2}m_l^{y_3}$.

Equations (4) and (5) are a set of coupled equations, also known as mean field equations. These equations are iteratively solved for a fixed point solution. Intuitively, parameters μ_{il} are updated by expected contributions from possible parents and neighbors, and similar for m_i^y. In (4) and (5), structure parameters μ_{il} depend on class label assignments, and m_i^y depend on expected structure connectivity. Thus, model structure selection is integrated with label assignment during the inference.

Now, we have presented a mean field approximation of the wake phase. To finish the sleep phase, the same mean field equations are enforced by coordinate descent alternating between observable variables Y_e and hidden variables S and Y_h. When first optimizing (5) for Y_e, the initial distribution of hidden variables are set as the optimal distribution at the end of wake phase. Then, take the optimal distribution of the former step as initial distribution of Y_e and optimize (4) and (5) to get an approximate distribution of hidden variables. For wake phase, initial distributions can be random and convergence is arrived at. But for sleep phase, a few steps are required to guarantee the improvement of CF_1^{App}.

2. $q(\mathrm{s}) = q(\mathrm{s_h}|\mathrm{s_v})q(\mathrm{s_v})$. Based on the assumption that $\mathrm{s_h}$ are deterministic and independent of $\mathrm{s_v}$, $q(\mathrm{s_h}|\mathrm{s_v})$ is an indicator function and takes all the probability one if $\mathrm{s_h}$ are the allowed connections.

Thus, all the terms in (1), (2), (4), and (5) can be calculated. The whole parameter estimation algorithm is as follows. First, apply (4) and (5) to iteratively compute the marginal probabilities of both wake and sleep phases. With the marginal probabilities, CF_1^{App} and its derivatives with respect to model parameters are calculated. Then, gradient-based optimization algorithms are applied to update model parameters. Here, we use the limited memory quasi-Newton method (Liu and Nocedal, 1989). The learning procedure is iterated until the relative change of CF_1^{App} is below some threshold. Although no guarantee exists that global optimization will be achieved, empirical studies show that this algorithm performs well.

For labeling a testing example, Equations (4) and (5) are iteratively solved with all variables free for a fixed point solution. At the end of convergence, the maximum a posterior model structure (a tree) is constructed from the probabilities μ_{il} by dynamic programming, and the most likely label assignments are found from the marginal probabilities m_i^y.

5. Implementation Details and Experimental Setup

Our experiments consist of two parts. The first part is to evaluate the performance of integrated web data extraction models compared with existing decoupled methods. The second part is to evaluate Dynamic Hierarchical Markov Random Fields (DHMRFs) compared with fixed-structured hierarchical models and Dynamic Trees (Williams and Adams, 1999). All the experiments are carried out on a real-world web data extraction task—production information extraction. In this section, we present the implementation details and the setup of our experiments. Results will be reported in the next two sections.

5.1 Features

As conditional models, DHMRFs and HCRFs can incorporate any useful feature for web data extraction. In this section, we present the types of features used in our experiments. As we shall note some of the features have been used in some existing extraction methods. However, they were mainly used as heuristic rules.

5.1.1 Features of Elements

For each element, we extract both content and visual features as listed in Table 1. All the features can be obtained through rendering a page. Previous work (Zhai and Liu, 2005; Zhu et al., 2005; Zhao et al., 2005; Gatterbauer et al., 2007) has shown the effectiveness of visual features for webpage analysis and information extraction.

5.1.2 Features of Blocks

The features of inner blocks are aggregations of their children's features. These features can be extracted via a bottom-up procedure starting from leaf nodes (or elements), such as the number of the children having a particular feature and the presence of a feature or a simultaneous presence of several features among the children. We also compute the following distances for each block to exploit the regularity of similar data records in a page.

Tree Distance Features: if two blocks are visually similar, usually their sub-trees on a vision-tree are also similar. We define the tree distance of two blocks as a measure of their structure similarity. The tree distance of two blocks is defined as the edit distance of their corresponding sub-

Name	Description
Content	The Content of a text element
Tag	The tag name of an element
Font Size	The font size of an element
Font Weight	The font weight of an element
Position	The coordinates of an element
Height	The height of an element's rectangle
Width	The width of an element's rectangle
Area	The area of an element's rectangle
Image URL	The source URL of an image element
Link URL	The action URL of an element if it exists
Image Alt-text	The alternative text of an image element

Table 1: The content and visual features of each element.

trees. Although the time-complexity of computing this distance could be high, we can substantially reduce the computation with some heuristics. For example, if the depth difference of two sub-trees is too large, they are not likely to be similar and this computation is not necessary. Once we have computed the tree distances, we can use some thresholds to define boolean-valued feature functions. For example, if the tree distance of two adjacent blocks is not more than 0.2, they are both likely to be data records.

Shape Distance and Type Distance Features: we also compute the shape distance and type distance (Zhao et al., 2005) of two blocks to exploit their similarity. For shape distance, we use the same definition of shape codes and the same calculation method as in the work (Zhao et al., 2005). To compute the type distance of two blocks, we define the following types for each element:

IMAGE: the element is an image.

JPEG IMAGE: the image element that is also a jpeg picture.

CODED IMAGE: the image element whose source URL contains at least three succeeding numbers, such as "/products/s_thumb/eb04iu_0190893_200t1.jpg".

TEXT: the element has text content.

LINK TEXT: the text element that contains an action URL.

DOLLAR TEXT: the text element that contains at least one dollar sign.

NOTE TEXT: the text element whose tag is "input", "select" or "option".

NULL: the default type of each element.

After defining each element's type code, a block's type code is defined as a sequence of the type codes of its children. As in the work by Zhao et al. (2005), multiple consecutive occurrences of each type are compressed to one occurrence. The edit distance of type codes is the type distance of two blocks.

Similar to the use of tree distance, we can easily incorporate shape distance and type distance by defining boolean-valued feature functions with pre-determined thresholds. Note that our model will not be sensitive to these thresholds because the defined feature functions are softened by learning a weight for each of them. Each feature function contributes its weight to the probability only when it is active. If a feature function is always active, it has no effect on the probability; and if a feature

Label Name	Semantic Meaning
Con_Image	Contains product's image
Con_Name	Contains product's name
Con_Price	Contains product's price
Con_Desc	Contains product's description
Con_ImgNam	Contains product's image and name
Con_NamPrc	Contains product's name and price
Con_ImgPrc	Contains product's image and price
Page Head	The head part of a Web page
Page Tail	The tail part of a Web page
Nav Bar	The navigation bar of a Web page
Data Region	Contains only similar data records
Data Record	Contains all the target attributes if exist
Info Block	Contains one or more data records and some additional information
Note Block	Contains no target attributes and are also not meaningful parts of a webpage

Table 2: Label spaces of inner variables for product information extraction.

function appears sparsely in the training set, smoothing techniques can be used to avoid over-fitting. Here, we use the spherical Gaussian prior to penalize the log-likelihood function during learning.

5.1.3 GLOBAL FEATURES

As described in the introduction, data records in the same webpage are always related. Based on work by Zhai and Liu (2005), we try to align the elements of two adjacent blocks in the same page and extract some global features to help attribute labeling.

For two neighboring blocks, we use the partial tree-alignment algorithm (Zhai and Liu, 2005) to align their elements. An alignment is discarded if most of the elements are not aligned. For successful alignments, the following feature is extracted.

Repeated elements are less informative: this feature is based on the observation that repeated elements in different records are more likely to be less useful, while important information such as the name of a product is not likely to repeat in the same webpage. For example, the "Add to cart" button appears in both data records as in Figure 1(a), but each record has a unique name. Currently, we just denote whether an element is repeated in different records. More complex measures like information entropy can be easily adopted. An example feature function can be defined as: if the element x_i repeatedly appears in the aligned records, it will be more likely to be labeled as Note or noise.

5.2 Label Spaces

For variables at leaf nodes, we are interested in deciding whether a leaf block (an element) is an attribute value of the object we want to extract. However, for variables at inner nodes, our interest shifts to the understanding of whether an inner block is a data record. So, we have two types of label spaces—leaf label space for variables at leaf nodes and inner label space for variables at inner nodes. The leaf label space consists of all the attribute names of the object we want to extract. In product information extraction, the leaf label space consists of *Name*, *Image*, *Price*, *Description*, and *Note*. *Note* is used to describe the data we are not interested in.

The inner label space can be partitioned into an object-type independent part and an object-type dependent part. We explain how to define these two parts in turn:

Object-type Independent Labels: Since we want to extract data from webpages, the labels *Page Head*, *Page Tail*, *Nav Bar*, and *Info Block* are naturally needed to denote different parts of a webpage. The labels *Data Record* and *Data Region* are also required for detecting data records. The label *Note Block* is also required to denote blocks that do not contain any meaningful information, such as the attributes to be extracted and the head, tail or navigation bar of a webpage. All these labels are general to any web data extraction problem, and they are independent of any specific object type.

Object-type Dependent Labels: Between data record blocks and leaf blocks, there are intermediate blocks on a vision-tree. So, we must define some intermediate labels between *Data Record* and the labels in the leaf label space. These labels are object-type dependent because intermediate blocks contain some object specific attribute values. A natural method is to use the combinations of the attributes to define intermediate labels. Of course, if we use all the possible combinations, the label space could be too large. We can discard unimportant combinations by considering the co-occurrence frequencies of their corresponding attribute values in the training data. The object-type dependent labels in product information extraction are listed in Table 2 with the format Con_*.

5.3 Data Sets

We set up two general data sets with randomly crawled product webpages. The list data set (*LDST*) contains 771 list pages and the detail data set (*DDST*) contains 450 detail pages. All the pages are parsed by VIPS and are hierarchically labeled, that is, every block in the parsed vision-trees is labeled. We use 200 list pages and 150 detail pages to learn the parameters of different models. The remaining pages (571 list pages and 300 detail pages) are used for testing. For each product item, we want to extract four attributes—*Name*, *Image*, *Price*, and *Description*.

For the training data, the detail pages are from 61 web sites and the list pages are from 81 web sites. The number of web sites that are found in both list and detail training data is 39. Thus, in total the training pages are taken from 103 different web sites. Totally, 58 unique templates are presented in the list training pages and 61 unique templates are presented in the detail training pages. For testing data, Table 3 shows the number of unique web sites where the pages come from and the number of different templates presented in these data. For example, the pages in *LDST* are from 167 web sites, of which 78 are found in list training data and 52 are found in detail training data. The number of web sites that are found in both list and detail training data is 34. Similar interpretation applies to other numbers in the table. Thus, totally 71 list page web sites and 263 detail page web sites are not seen in the training data. For templates, 83 list page templates and 208 detail page templates are not seen the training data. For different templates, the number of documents varies. In *LDST*, most of the templates have 2 to 5 documents. In *DDST*, pages from different web sites typically have different templates and thus most templates have 1 document.

5.4 Evaluation Metrics

For data record detection, we use the standard *P*recision, *R*ecall and *F1* measure to evaluate the methods. A block is considered as a correctly detected data record if it contains all the appeared

Data Sets	*LDST*	*DDST*
#Web Site	167 (78/52/34)	268 (2/3/0)
#Template	140 (57/0/0)	212 (0/4/0)

Table 3: Statistics of the data sets.

attributes of one object, and does not contain any attributes of other objects. A correct data record could tolerate (miss or contain) some non-important information like "Add to Cart" button.

For attribute labeling, the performance on each attribute is evaluated by *P*recision (the percentage of returned elements that are correct), *R*ecall (the percentage of correct elements that are returned), and their harmonic mean *F1*. We also use two comprehensive evaluation criteria:

Block Instance Accuracy (Blk_IA): the percentage of data records of which the key attributes (*Name*, *Image*, and *Price*) are all correctly labeled.

Average F1 (Avg_F1): the average of F1 values of different attributes.

6. Evaluation of Integrated Web Data Extraction Models

In this section, we report the evaluation results of integrated web data extraction models compared with decoupled models. The results demonstrate that integrated extraction models can achieve significant improvements over decoupled models in both record detection and attribute labeling. We also show the generalization ability of the integrated extraction models.

6.1 Methods

We build the baseline methods by sequentially combining the record detection algorithm DEPTA (Zhai and Liu, 2005) and 2D CRFs (Zhu et al., 2005). For detail pages, which DEPTA cannot deal with, we first detect the main data block using the method by Song et al. (2004) and then use 2D CRFs to perform attribute labeling on the detected main block. For the integrated extraction model, a webpage is first segmented by VIPS to construct a vision-tree and then HCRFs are used to detect both records and attributes on the vision-tree. Note that all the HCRFs evaluated in this section are the model in Figure 3(b). The evaluation results of another HCRFs, which are slightly better, are presented in Section 7.

To see the effect of the global features in Section 5.1.3, we also evaluate an HCRF model that does not use these global features. We denote this model by H_NG (without global features). Similarly, we evaluate two 2D CRF models in the baseline methods. As in the work of Zhu et al. (2005), a basic 2D CRF model is set up with only the basic features (see Table 1) when labeling each detected data record. Another 2D CRF model is set up with both the basic features and the global features. We denote the basic model by 2D CRF and denote the other model by 2D_G. For 2D_G, we first cache all the detected records from one webpage and then extract the global features. As there is no tree structure here, the alignments are based on the elements' relative positions in each record.

To see the separate effect of our approach on record detection and attribute labeling, we first detect data records on the parsed vision-trees using the content features, tree distance, shape distance, and type distance features. Then, we use HCRFs to label the detected records. When doing attribute labeling, we also evaluate two HCRF models with and without the global features. These two models are denoted by H_S and H_SNG respectively.

For all the HCRF models, we use 200 list pages and 150 detail pages together to learn their parameters. We use the same 200 list pages to train a 2D CRF model for extraction on list pages, and use the same 150 detail pages to train another 2D CRF model for extraction on detail pages. The reason for training two models for list and detail pages separately is that, for a 2D CRF model, the features and parameters for list and detail pages are quite different and a uniform model cannot work well. In the training stage, all of the algorithms converge quickly, within 20 iterations.

6.2 Results and Discussions

We compare our approach with DEPTA (Zhai and Liu, 2005) on *LDST* for data record detection. The running results of DEPTA on our data set are kindly provided by its authors. DEPTA has a similarity threshold, and it is set at 60% in this experiment. Some simple heuristics are also used in DEPTA to remove some noise records. For example, a data region that is far from the center or contains neither image nor dollar sign is removed.

6.2.1 RECORD DETECTION

The results of record detection are shown in Table 4. We can see that both HCRF and H_NG significantly outperform DEPTA in recall, improved by 8.1 points, and precision, improved by 7.5 points. The improvements come from two parts:

Advanced data representation and more features: in our model, we incorporate more features such as content features and shape distance and type distance features than DEPTA. We also adopt an advanced representation of webpages—vision-trees which have been shown to outperform tag-tree representation(Cai et al., 2004). As we can see from Table 4, H_SNG and H_S outperform DEPTA, and we gain about 2 points in precision, 7.3 points in recall, and 4.6 points in F1.

Incorporation of semantics during record detection: DEPTA just detects the blocks with regular patterns (i.e., regular tree structures) and does not take semantics into account. Thus, although some heuristics are used to remove some noise blocks, the results still contain blocks that are not data records or just parts of data records. In contrast, our approach integrates attribute labeling into block detection and can consider semantics during detecting data records. So, the blocks detected are of better quality and are more likely to be data records. For instance, a block containing a product's name, image, price and some descriptions is almost certain to be a data record, but a block containing only irrelevant information is unlikely to be a data record. The lower precisions of H_SNG and H_S demonstrate this. When not considering the semantics of the elements, H_SNG and H_S extract more noise blocks compared with H_NG or HCRF, so the precisions of record detection decrease by 5.5 points and the overall F1 measures decrease by 3.2 points.

6.2.2 ATTRIBUTE LABELING

As we can see from Table 5, our HCRF model significantly outperforms the baseline approach. On list pages, H_NG gains 18.7 points over 2D CRF in block instance accuracy and the achievements of HCRF are 13.9 points higher when compared with 2D CRF_G. On detail pages, our approach gains about 58 points over 2D CRF in block instance accuracy. The reasons for the better performance are:

Models	*H_SNG*	*H_S*	*H_NG*	*HCRF*	*DEPTA*
P	0.904	0.904	**0.959**	**0.959**	0.884
R	0.921	0.921	**0.930**	**0.930**	0.849
F1	0.912	0.912	**0.944**	**0.944**	0.866

Table 4: Record detection results of different methods on *LDST*.

Data Sets		LDST						DDST	
Models		*H_SNG*	*H_S*	*H_NG*	*HCRF*	*2D CRF*	*2D_G*	*HCRF*	*2D CRF*
P	Name	0.836	0.860	0.880	**0.911**	0.763	0.851	**0.835**	0.398
	Image	0.901	0.905	0.952	**0.966**	0.842	0.838	**0.978**	0.546
	Price	0.906	0.903	0.959	**0.963**	0.913	0.915	**0.986**	0.809
	Desc	0.783	0.766	**0.792**	0.788	0.769	0.779	**0.663**	0.588
R	Name	0.851	0.875	0.854	**0.882**	0.735	0.822	**0.761**	0.398
	Image	0.917	0.921	0.924	**0.936**	0.811	0.809	**0.892**	0.546
	Price	0.922	0.919	0.930	**0.933**	0.879	0.883	**0.899**	0.809
	Desc	**0.797**	0.780	0.768	0.764	0.741	0.752	**0.604**	0.395
F1	Name	0.843	0.867	0.867	**0.896**	0.749	0.836	**0.796**	0.398
	Image	0.909	0.913	0.938	**0.951**	0.826	0.823	**0.933**	0.546
	Price	0.914	0.911	0.944	**0.948**	0.896	0.899	**0.940**	0.809
	Desc	**0.790**	0.773	0.780	0.776	0.755	0.765	**0.632**	0.473
Avg_F1		0.864	0.866	0.882	**0.893**	0.807	0.831	**0.825**	0.556
Blk_IA		0.789	0.816	0.856	**0.890**	0.669	0.751	**0.817**	0.231

Table 5: Attribute labeling results of different methods on both *LDST* and *DDST*, where *Desc* stands for *Description*.

Attribute labeling benefits from good quality records: one reason for this better performance is that attribute labeling can benefit from the good results of record detection. For example, if a detected record is not a data record or misses some important information such as *Name*, attribute labeling will fail to find the missed information or will find some incorrect information. So, H_SNG outperforms 2D CRF and H_S outperforms 2D_G. Of course the achievements of H_SNG and H_S may also come from the incorporation of long distance dependencies, which will be discussed later.

Global features help attribute labeling: another reason for the improvements in attribute labeling is the incorporation of the global features as in Section 5.1.3. From the results, we can see that when considering global features, attribute labeling is more accurate. For example, 3.4 points are gained in block instance accuracy by HCRF compared with H_NG, and H_S achieves 2.7 points in block instance accuracy compared with H_SNG. For the two baseline methods, compared with 2D CRF, which uses only the features of the elements in each detected record, more than 8 points are gained in block instance accuracy by 2D_G, which incorporates the global features.

HCRF models incorporate long distance dependencies: the third reason is the incorporation of long distance dependencies. From the results, we can see that hierarchical models could get promising results while 2D CRFs perform poorly on detail pages. This is because, for a detected record, 2D CRFs put its elements in a two-dimensional grid and long distance interactions cannot be incorporated in the flat model, due to the first-order Markov assumption. In contrast, HCRF models can incorporate dependencies at various levels and thus incorporate long distance dependencies. For detail pages, as there is no record detection, H_SNG and H_S are not applicable here. There are no global features either, so we just list the results of HCRF and 2D CRF in Table 5.

The quite different performance of 2D CRFs on list and detail pages says the same thing about the effectiveness of long distance dependencies. For list pages, the inputs are data records, which always contain a small number of elements. In this case, 2D CRFs can effectively model the dependencies of the attributes and achieve reasonable accuracy. Note that the results on detail pages are achieved without any pre-processing to remove noise elements. Empirical studies show that some appropriate pre-processing can improve the performance significantly on detail pages.

6.3 Generalization Ability

We report some empirical results to show the generalization ability of the integrated web data extraction models. We randomly pick 37 templates from *LDST* and for each template we collect 5 webpages for training and 10 webpages for testing. We randomly select $N (N = 1, 2, 3, \cdots, 37)$ templates together with their training pages as training data, and test the model on all the testing webpages of the 37 templates. For each N, we run the integrated HCRFs 10 times and take the average as the final results. Figure 5 shows the average F1 and block instance accuracy against different N. We can see that the integrated extraction models converge very quickly. As the number of templates increase in the training data, the extraction accuracy becomes higher and the variances become smaller. The strong generalization ability to unseen templates is mainly due to the very general and robust visual features we are using in our models. For different templates, although the low-level HTML codes or HTML tag trees are quite different, the visual layout and visual features they use are usually common. Thus, we can learn a robust model from a small set of templates and generalize well to unseen templates. Section 7.3 presents another set of results that show the generalization ability to unseen templates.

7. Evaluation of Dynamic Hierarchical Markov Random Fields

In this section, we report the evaluation results of Dynamic Hierarchical Markov Random Fields compared with fixed-structured hierarchical models and Dynamic Trees. Results show that DHMRFs can (at least partially) overcome the blocky artifact issue in diverse web data extraction. We also present some empirical studies about the learning algorithm of DHMRFs.

7.1 Models

We compare DHMRFs with HCRFs in both Figure 3(b) and 3(c), Dynamic Trees (D-Trees), and fixed-structured tree models (F-Trees). For HCRFs and F-Trees, all training pages are hierarchically labeled. The training is complete and exact message passing algorithms are used to learn their parameters and find MAP label assignments. For DHMRFs and D-Trees, labels of leaf nodes are kept the same and inner labels are hidden during learning. For the incomplete training, we apply the variational method developed in this paper for DHMRFs. Mean field approximation is also used for Dynamic Trees. For DHMRFs and HCRFs, the same set of feature functions are used for class

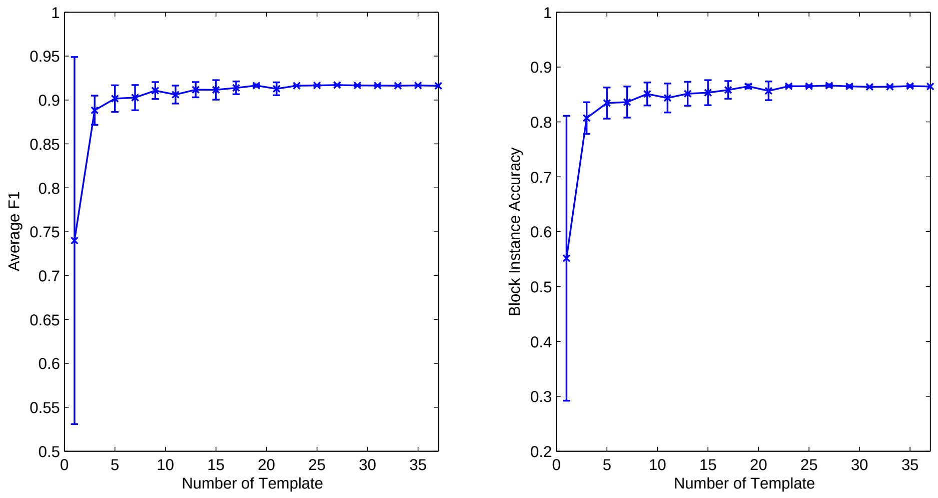

Figure 5: The left plot is the mean and variance of the Average F1 and the right plot is the mean and variance of the Block Instance Accuracy.

label assignment. We will use *HCRF* and *HCRF+* to denote the two HCRF models in Figure 3(b) and 3(c) respectively.

To apply DHMRFs and D-Trees, initial configuration of the model structure must be carried out first. Basically, we need to initially set the number of layers and the number of nodes at each layer. It may be different for different application domains to set the initial configuration. For image processing, it can be done via sub-sampling or wavelet filtering. For web data extraction, the data are represented as texts, images, buttons, and so on. These atomic information units are more expressive compared to image pixels. There is definitely no benefit to view a webpage as a collection of image pixels and then apply the methods in image processing. Here, we use the same number of layers (and the same number of nodes at each layer) in dynamic models as in the vision-trees. Note that additional nodes can be introduced. For DHMRFs feature functions can be easily defined to consider these nodes, and for D-Trees the *part-time-node-employment* prior (Adams and Williams, 1999) can be applied to get a sparse structure.

For D-Trees, two sets of parameters—conditional probability tables (CPTs) and affinities, need to be set. We keep the affinities fixed and learn the CPTs. To avoid over-parametrization, layer-wise CPT sharing is adopted in previous work. However, for heterogeneous web data, three-layer-wise sharing is better. That is, every three layers from the top down share one CPT. To incorporate evidence, we use the class-independent model (Storkey and Williams, 2003) with emission distributions set as the empirical frequencies in the training data set. CPTs are also initialized as frequencies. To avoid zero probabilities of unseen samples, Laplace's rule is used with pseudocount set at one. Our study shows that when the affinities are set as 0 for the natural parent, -1 for the nearest neighbors of the natural parent, and -3 for the null parent, better performance is achieved compared to previously used settings. The CPTs used in our experiments are achieved with 10 iterations.

7.2 Extraction Accuracy

Table 6 shows the extraction accuracy of different models. From the results, we can see that DHMRFs achieve the highest performance on both data sets. Compared to the fixed *HCRF*, on *LDST* about 3 points in Average F1 and about 5 points in Block Instance Accuracy are gained. Compared to the more complex *HCRF+*, more than 2 points in Average F1 and about 3 points in Block Instance Accuracy are achieved. More specifically, compared to *HCRF+*, more than 3 points are achieved in both precision and recall on *Name*, and more than 2 points are achieved on *Desc*. For *Image* and *Price* the improvements are smaller. This is because *Image* and *Price* are usually more distinctive than the other attributes. So both models perform quite well. On *DDST*, the improvements in *Name* are about 4 points in both precision and recall, and for *Description* the improvements are about 7 points in both precision and recall. Small improvements are achieved in *Image* and *Price* due to the same reason as in list pages.

The improvements demonstrate the merits of DHMRFs. First, DHMRFs can incorporate the two-dimensional neighborhood dependencies among the nodes at the same level, which have been shown to be useful (Zhu et al., 2005). The better performance of *HCRF+* compared to *HCRF* also shows the usefulness of two-dimensional neighborhood dependencies. By dynamically selecting connections between different nodes, DHMRFs can bring together the attributes of the same object (here, an object is a product item), and thus the correlation between these attributes can be strengthened. Second, DHMRFs can deal with webpages with intertwined attributes (Zhai and Liu, 2005). For these webpages, the attributes of different objects are intertwined in HTML tag trees. Unaware of semantic labels, the constructed vision-trees also have intertwined attributes. In these cases, fixed-structured HCRFs (both *HCRF* and *HCRF+*) cannot correctly detect data records by simply assigning labels to the nodes of a vision-tree. Instead, as structure selection is integrated with labeling in DHMRFs, the dynamic model can properly group the attributes of the same object, and at the same time separate the attributes of different objects with the help of semantic labels. The semantic labels have been shown to be helpful in detecting data records (i.e., groups of attributes) in previous experiments. Note that although intertwined cases are usually fewer than non-intertwined cases, they are not sparse samples in our model. This is because although their edge connections in HTML tag trees are somewhat different from non-intertwined ones, the visual features they share are almost the same. Thus, training samples with or without intertwined cases can teach a good model. In fact, to keep it fair for both dynamic models and fix-structured models, we only provide non-intertwined samples during training.

Compared to the fixed F-Trees, the worse performance of D-Trees is quite counter-intuitive. However, a close examination of the results reveals that the reason for the worse performance is due to the less discriminative power of D-Trees. As we have stated, for diverse web data CPT sharing can be difficult. Although empirical studies can find a good sharing method, we couldn't learn an optimal model with a limited set of training samples. Furthermore, its generative characteristic causes difficulty in encoding useful features. In this way, more uncertainty in structure selection couldn't be resolved than that in DHMRFs. This is evident if we look at the average log-likelihood of the MAP connections over all samples and all nodes. For D-Trees the average value is -0.4080, and for DHMRFs it is -0.3170. In terms of probability, they are equivalent to 0.6650 and 0.7283 respectively. The less discriminative power of D-Trees causes additional errors in constructing model structures even for the non-intertwined cases, and thus hurts the accuracy of record detection and attribute labeling. So, D-Trees perform worse than F-Trees, which can deal with the non-

Data Sets		LDST					DDST				
Models		*F-Tree*	*D-Tree*	*HCRF*	*HCRF+*	*DHMRF*	*F-Tree*	*D-Tree*	*HCRF*	*HCRF+*	*DHMRF*
P	Name	0.890	0.879	0.911	0.920	**0.952**	0.829	0.785	0.835	0.835	**0.874**
	Image	0.959	0.951	0.966	0.968	**0.988**	0.972	0.928	**0.978**	**0.978**	**0.978**
	Price	0.960	0.937	0.963	0.972	**0.978**	0.976	0.947	0.986	**0.990**	0.989
	Desc	0.804	0.800	0.788	0.805	**0.828**	0.722	0.698	0.663	0.656	**0.730**
R	Name	0.842	0.744	0.882	0.897	**0.928**	0.779	0.684	0.761	0.753	**0.799**
	Image	0.908	0.805	0.936	0.944	**0.958**	0.868	0.809	0.892	0.883	**0.898**
	Price	0.910	0.794	0.936	**0.951**	0.949	0.888	0.826	0.899	0.893	**0.905**
	Desc	0.762	0.678	0.764	0.786	**0.811**	0.641	0.609	0.604	0.603	**0.668**
F1	Name	0.865	0.806	0.896	0.908	**0.940**	0.803	0.731	0.796	0.792	**0.835**
	Image	0.933	0.872	0.951	0.956	**0.973**	0.917	0.864	0.933	0.928	**0.936**
	Price	0.934	0.860	0.948	0.961	**0.963**	0.930	0.882	0.940	0.939	**0.945**
	Desc	0.782	0.734	0.776	0.795	**0.819**	0.679	0.650	0.632	0.628	**0.698**
Avg_F1		0.879	0.818	0.893	0.902	**0.924**	0.832	0.782	0.825	0.822	**0.854**
Blk_IA		0.869	0.837	0.890	0.912	**0.940**	0.809	0.762	0.817	0.819	**0.853**

Table 6: Extraction accuracy on *LDST* and *DDST*, where *Desc* stands for *Description*.

intertwined cases well. The results also show that the directed tree models can perform well on our data sets, but are inferior to HCRFs.

7.3 Extraction Accuracy on Unseen Templates

For detail pages, since only a small number (i.e., 4) of templates in the testing data are seen in the training data, the results on webpages generated from unseen templates do not change much. Here, we only report the results on list pages. In total, *LDST* has 83 templates that are not seen in the training data. We select out all the pages with unseen templates, the total number being 190. Figure 6 shows the results of our models on these webpages. The overall performance is still very promising although it is lower than that on the whole set of webpages. Generally, the Dynamic Hierarchical Markov Random Fields always outperform all the other models. The integrated HCRFs outperform the sequential HCRFs, which take record detection and attribute labeling as two separate steps as described in Section 6.1. Dynamic Trees achieved the worst results due to the same reason of a less discriminative power in structure selection.

7.4 Fitness of Model Structure

Figure 7(a) compares the posterior probabilities of the MAP structures constructed by DHMRFs with those of the fixed structures. In terms of the number of nodes, the sizes of webpages change from 39 to 576 (average 166) in *LDST*, and the log posteriors change from -503.80 to -4.49 (average -50.7). In *DDST*, sizes range from 14 to 705 (average 131), and log posteriors range from -184.40 to -1.72 (average -42.47). Here, we only present the samples whose log posteriors are between -200 and 0 because most of the samples ($> 97\%$) fall into this interval. We can see that the MAP structures by DHMRFs always appear above the equal probability line. Thus, the structures found by the dynamic

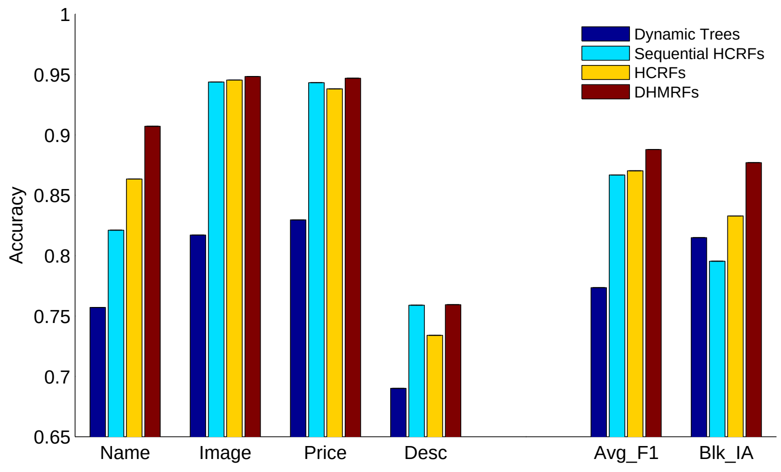

Figure 6: The performance of Dynamic Trees, Sequential HCRFs, HCRFs, and DHMRFs on the webpages whose templates are not presented in the training data. From left to right, the first four groups of the columns are the F1 of different attributes.

model have higher posterior probabilities. Another observation is that the distribution of samples from *DDST* is more disperse than that of the samples from *LDST*. The reason is that in list pages the attributes of an object always concentrate into small clusters, while they can scatter anywhere in detail pages.

7.5 Study about the Inference Algorithm

Figure 7(b) shows the change of average contrastive divergence with respect to iteration numbers in the learning of DHMRFs. To initialize the algorithm, at the wake phrase m_i^y are set to a uniform distribution plus a Gaussian noise with zero mean and variance 0.01, and μ_{il} are set to a random distribution. The model weights are initialized to zero. We can see that before 7 iterations average contrastive divergence decreases stably. And after 7, slight disturbances appear. But as for extraction accuracy, marginal changes occur (no more than 0.5 point in Block Instance Accuracy). Thus, the learning algorithm is quite stable. All the above results are achieved at iteration 7. The same initialization is used in labeling, and by running both learning and labeling many times, we observe that the algorithm is insensitive to the random initialization. Since the mean field equations are locally calculated and their update can typically converge within 5 iterations, both the learning and labeling are efficient.

8. Conclusions and Future Work

In this paper, we proposed an integrated web data extraction paradigm with hierarchical models. The proposed model is called Dynamic Hierarchical Markov Random Fields (DHMRFs), which take fixed-structured Hierarchical Conditional Random Fields (HCRFs) as a special case. DHMRFs incorporate structural uncertainty in a discriminative manner. By dynamically selecting connections

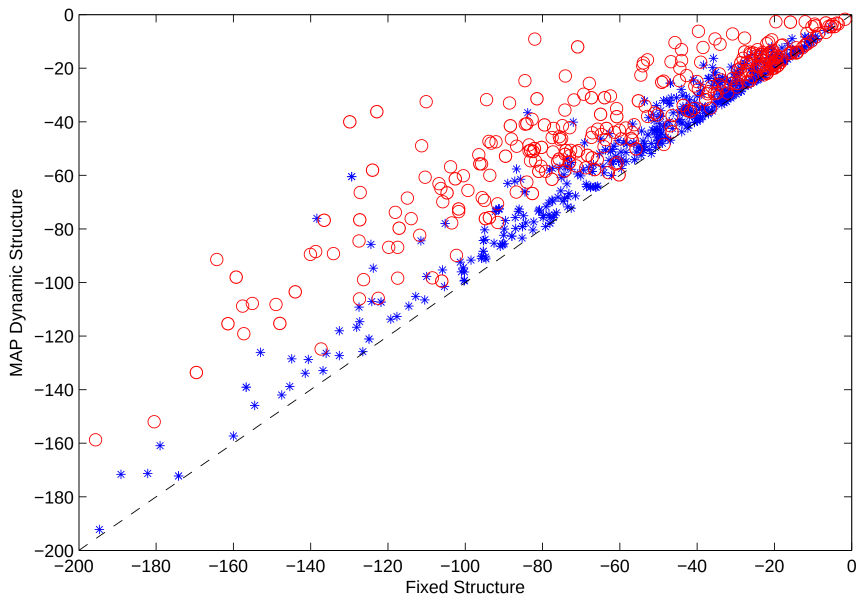

(a)

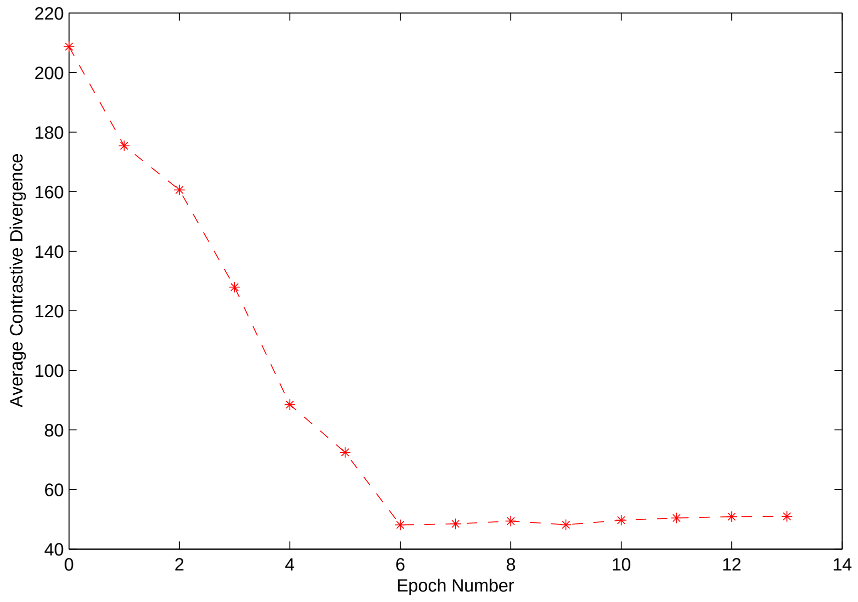

(b)

Figure 7: (a) The log posteriors of MAP dynamic structures against those of fixed structures. Samples in asterisks are from *LDST* and those in circles are from *DDST*; (b) The change of average contrastive divergence with respect to iteration numbers.

between variables, DHMRFs can potentially address the blocky artifact issue in diverse web data extraction. Compared to directed models, DHMRFs are compact in representation and powerful in encoding useful features. We develop a contrastive divergence learning algorithm to learn the parameters for DHMRFs. For the special case—HCRFs, parameter learning can be exactly performed with some assumption about the linearity of the neighborhood dependencies among sibling nodes, and without such an assumption piecewise learning can be applied to achieve a good approximation. We apply the models to a real-world web data extraction task. Experimental results show that: (1) integrated extraction models perform significantly better than decoupled methods on both record detection and attribute labeling; (2) DHMRFs can potentially address the blocky artifact issue in diverse web data extraction; (3) integrated extraction models can generalize well to unseen templates.

In our experiments, we apply a simple method to select labels for inner variables according to the co-occurrence frequency. Apparently, labels should not be selected independently and methods considering the correlations between different labels could be more desirable. We plan to try advanced methods in the future. It is also interesting to develop models that can automatically discover the number of layers and the number of nodes at each layer. Finally, extensive studies of the integrated extraction models in other complicated domains, like extracting researchers' information (Zhu et al., 2007a), is also to comprise our future work.

Acknowledgments

We thank the anonymous reviewers for helpful comments in improving the earlier version of the paper. The authors Jun Zhu and Bo Zhang are supported by National Natural Science Foundation of China under the Grant No. 60621062, and National Key Foundation R&D Project under the Grant No. 2003CB317007 and 2004CB318108.

References

Nicholas J. Adams and Christopher K. I. Williams. SDTs: Sparse dynamic trees. In *Artificial Neural Networks*, 1999.

Arwind Arasu and Hector Garcia-Molina. Extracting structured data from webpages. In *Proc. of the International Conference on Management of Data*, San Diego, CA, 2003.

David Buttler, Ling Liu, and Calton Pu. A fully automated object extraction system for the world wide web. In *Proc. of International Conference on Distributed Computing Systems*, Arizona, USA, 2001.

Deng Cai, Shipeng Yu, Ji-Rong Wen, and Wei-Ying Ma. Block-based web search. In *Proc. of the Internaltinoal Conference on Information Retrieval*, Sheffield, UK, 2004.

Miguel A. Carreira-Perpinan and Geoffrey E. Hinton. On contrastive divergence learning. In *Proc. of Artificial Intelligence and Statistics*, Barbados, 2005.

Chia-Hui Chang and Shao-Chen Lui. IEPAD: Information extraction based on pattern discovery. In *Proc. of the International World Wide Web Conference*, Hong Kong, China, 2001.

Robert G. Cowell, A.Philip Dawid, Steffen L. Lauritzen, and David J. Spiegelhalter. *Probabilistic Networks and Expert Systems*. Springer, New York, NY, 1999.

Valter Crescenzi, Giansalvatore Mecca, and Paolo Merialdo. ROADRUNNER: Towards automatic data extraction from large web sites. In *Proc. of the Conference on Very Large Data Bases*, Rome, Italy, 2001.

Aron Culotta, Trausti Kristjansson, Andrew McCallum, and Paul Viola. Corrective feedback and persistent learning for information extraction. *Artificial Intelligence Journal*, 170(14):1101–1122, 2006.

David W. Embley, Y. Jiang, and Y.-K. Ng. Record-boundary discovery in web documents. In *Proc. of the International Conference on Management of Data*, Philadephia, PA, 1999.

Wolfgang Gatterbauer, Paul Bohunsky, Marcus Herzog, Bernhard Krupl, and Bernhard Pollak. Towards domain-independent information extraction from web tables. In *Proc. of the International World Wide Web Conference*, Banff, Canada, 2007.

Lise Getoor, Nir Friedman, Daphne Koller, and Benjamin Taskar. Learning probabilistic models of relational structure. In *Proc. of the International Conference on Machine Learning*, Williams College, Williamstown, MA, 2001.

Xuming He, Richard S. Zemel, and Miguel A. Carreira-Perpinan. Multiscale conditional random fields for image labeling. In *IEEE Conference on Computer Vision and Pattern Recognition*, Washington, DC, 2004.

Geoffrey E. Hinton. Training products of experts by minimizing contrastive divergence. *Neural Computation*, 14(8):1771–1800, 2002.

William W. Irving, Paul W. Fieguth, and Alan S. Willsky. An overlapping tree approach to multiscale stochastic modeling and estimation. *IEEE Trans. on Image Processing*, 6(11):1517–1529, 1997.

Michael I. Jordan, Zoubin Ghahramani, Tommis Jaakkola, and Lawrence K. Saul. *An Introduction to Variational Methods for Graphical Models*. M. I. Jordan (Ed.), Learning in Graphical Models, Cambridge: MIT Press, Cambridge, MA, 1999.

Zoltan Kato, Marc Berthod, and Josiane Zerubia. Multiscale Markov random field models for parallel image classification. In *IEEE International Conference on Computer Vision*, Berlin, Germany, 1993.

Sanjiv Kumar and Martial Hebert. A hierarchical field framework for unified context-based classification. In *IEEE International Conference on Computer Vision*, Beijing, China, 2005.

Nicholas Kushmerick. Wrapper induction: efficiency and expressiveness. *Artificial Intelligence*, 118:15–68, 2000.

John Lafferty, Andrew McCallum, and Fernando Pereira. Conditional random fields: Probabilistic models for segmenting and labeling sequence data. In *Proc. of the International Conference on Machine Learning*, Williams College, Williamstown, MA, 2001.

Kristina Lerman, Lise Getoor, Steven Minton, and Craig Knoblock. Using the structure of web sites for automatic segmentation of tables. In *Proc. of the International Conference on Management of Data*, Paris, France, 2004.

Jia Li, Robert M. Gray, and Richard A. Olshen. Multiresolution image classification by hierarchical modeling with two-dimensional hidden Markov models. *IEEE Trans. on Information Theory*, 46 (5):1826–1841, 2000.

Lin Liao, Dieter Fox, and Henry Kautz. Location-based activity recognition. In *Advances in Neural Information Processing Systems*, Whistler, Canada, 2005.

Dong C. Liu and Jorge Nocedal. On the limited memory bfgs method for large scale optimization. *Mathematical Programming*, 45:503–528, 1989.

Ion Muslea, Steven Minton, and Craig A. Knoblock. Hierarchical wrapper induction for semi-structured information sources. *Journal of Autonomous Agents and Multi-Agent*, 4(1-2):93–114, 2001.

Ariadna Quattoni, Michael Collins, and Trevor Darrell. Conditional random fields for object recognition. In *Advances in Neural Information Processing Systems*, Vancouver, Canada, 2004.

Garry Robins, Pip Pattison, Yuval Kalish, and Dean Lusher. An introduction to exponential random graph ($p^\star$) model for social networks. *Social Networks*, 2006.

Ruihua Song, Ji-Rong Wen, and Wei-Ying Ma. Learning block importance models for web pages. In *Proc. of the International World Wide Web Conference*, Budapest, Hungary, 2004.

Amos J. Storkey and Christopher K. I. Williams. Image modeling with position-encoding dynamic trees. *IEEE Trans. on Pattern Analysis and Machine Intelligence*, 25(7):859–871, 2003.

Charles Sutton and Andrew McCallum. Piecewise training for undirected models. In *Uncertainty in Artificial Intelligence*, Edinburgh, Scotland, 2005.

Charles Sutton, Khashayar Rohanimanesh, and Andrew McCallum. Dynamic conditional random fields: factorized probabilistic models for labeling and segmenting sequence data. In *Proc. of the International Conference on Machine Learning*, Banff, Canada, 2004.

Sinisa Todorovic and Michael C. Nechyba. Dynamic trees for unsupervised segmentation and matching of image regions. *IEEE Trans. on Pattern Analysis and Machine Intelligence*, 27(11): 1762–1777, 2005.

Martin Wainwright, Tommi Jaakkola, and Alan Willsky. A new class of upper bounds on the log partition function. In *Uncertainty in Artificial Intelligence*, Alberta, Canada, 2002.

Max Welling and Geoffrey E. Hinton. A new learning algorithm for mean field boltzmann machines. In *International Conference on Artificial Neural Networks*, Vienna, Austria, 2001.

Max Welling and Charles Sutton. Learning in Markov random fields with contrastive free energies. In *Artificial Intelligence and Statistics*, Barbados, 2005.

Christopher K. I. Williams and Nicholas J. Adams. DTs: dynamic trees. In *Advances in Neural Information Processing Systems*, Denver, Colorado, USA, 1999.

Alan S. Willsky. Multiresolution Markov models for signal and image processing. In *Proc. of the IEEE*, 2002.

Alan L. Yuille. The convergence of contrastive divergence. In *Advances in Neural Information Processing Systems*, Vancouver, Canada, 2004.

Yanhong Zhai and Bing Liu. Web data extraction based on partial tree alignment. In *Proc. of the International World Wide Web Conference*, Chiba, Japan, 2005.

Hongkun Zhao, Weiyi Meng, Zonghuan Wu, Vijay Raghavan, and Clement Yu. Fully automatic wrapper generation for search engines. In *Proc. of the International World Wide Web Conference*, Chiba, Japan, 2005.

Jun Zhu, Zaiqing Nie, Ji-Rong Wen, Bo Zhang, and Wei-Ying Ma. 2D conditional random fields for web information extraction. In *Proc. of the International Conference on Machine Learning*, Bonn, Germany, 2005.

Jun Zhu, Zaiqing Nie, Ji-Rong Wen, Bo Zhang, and Wei-Ying Ma. Simultaneous record detection and attribute labeling in web data extraction. In *Proc. of the International Conference on Knowledge Discovery and Data Mining*, Philadelphia, PA, 2006.

Jun Zhu, Zaiqing Nie, Ji-Rong Wen, Bo Zhang, and Hsiao-Wuen Hon. Webpage understanding: an integrated approach. In *Proc. of the International Conference on Knowledge Discovery and Data Mining*, San Jose, CA, 2007a.

Jun Zhu, Zaiqing Nie, Bo Zhang, and Ji-Rong Wen. Dynamic hierarchical Markov random fields and their application to web data extraction. In *Proc. of the International Conference on Machine Learning*, Corvallis, OR, 2007b.